JAAS

Sample preparation with sucrose cryoprotection dramatically alters Zn distribution in the rodent hippocampus, as revealed by elemental mapping

Journal:	*Journal of Analytical Atomic Spectrometry*
Manuscript ID	JA-TEC-07-2020-000323.R1
Article Type:	Technical Note
Date Submitted by the Author:	12-Aug-2020
Complete List of Authors:	Pushie, M. Jake; University of Saskatchewan, Department of Surgery, Division of Neurosurgery, College of Medicine Hollings, Ashley; Curtin University, School of Molecular and Life Sciences; Curtin University, Curtin Health Innovation Research Institute Reinhardt, Juliane; Australian Nuclear Science and Technology Organisation Webb, Samuel; Stanford Synchrotron Radiation Lightsource, SLAC National Accelerator Laboratory Lam, Virginie; Curtin University, Curtin Health Innovation Research Institute; Curtin University, School of Public Health, Faculty of Health Sciences Takechi, Ryu; Curtin University, Curtin Health Innovation Research Institute; Curtin University, School of Public Health, Faculty of Health Sciences Mamo, J.C.L.; Curtin University, Curtin Health Innovation Research Institute; Curtin University, School of Public Health, Faculty of Health Sciences Paterson, Phyllis; University of Saskatchewan, College of Pharmacy and Nutrition Kelly, Michael; University of Saskatchewan, Department of Surgery, Division of Neurosurgery, College of Medicine George, Graham; University of Saskatchewan, School Molecular and Environmental Sciences Group, Geological Sciences; University of Saskatchewan, Department of Chemistry Pickering, Ingrid; University of Saskatchewan, School Molecular and Environmental Sciences Group, Geological Sciences; University of Saskatchewan, Department of Chemistry Hackett, Mark; Curtin University, School of Molecular and Life Sciences; Curtin University, Curtin Health Innovation Research Institute

Sample preparation with sucrose cryoprotection dramatically alters Zn distribution in the rodent hippocampus, as revealed by elemental mapping

Pushie, M.J.,[1] Hollings, A.,[2,3] Reinhardt J.,[4] Webb, S.M.,[5] Lam, V.,[2,6] Takechi, R.,[2,6] Mamo, J.C.,[2,6] Paterson, P.G.,[7] Kelly, M.E.,[1] George, G.N.,[8] Pickering, I.J.,[8] Hackett, M.J.*[2,3]

1. Department of Surgery, Division of Neurosurgery, College of Medicine, University of Saskatchewan, 107 Wiggins Road, Saskatoon, Saskatchewan S7N 5E5, Canada
2. Curtin Health Innovation Research Institute, Curtin University, Perth, WA 6102, AUS
3. School of Molecular and Life Sciences, Curtin University, Perth, WA 6845, AUS
4 Australian Nuclear Science and Technology Organisation, 800 Blackburn Road, Clayton, VIC, AUS 3168
5. Stanford Synchrotron Radiation Lightsource, SLAC National Accelerator Laboratory, Menlo Park, California, USA 94025
6. School of Public Health, Faculty of Health Sciences, Curtin University, WA, Australia
7. College of Pharmacy and Nutrition, University of Saskatchewan, 107 Wiggins Rd, Saskatoon, Saskatchewan, S7N 5E5, Canada
8. School Molecular and Environmental Sciences Group, Geological Sciences, University of Saskatchewan, 114 Science Place, Saskatoon, Saskatchewan S7N 5E2, Canada
9. Department of Chemistry, University of Saskatchewan, 110 Science Place, Saskatoon, Saskatchewan S7N 5C9, Canada

* Corresponding Author:　　E-mail: mark.j.hackett@curtin.edu.au　　　　Tel.: +61 8 9266 3102

KEY WORDS: Zn, hippocampus, XFM, LA-ICP-MS, metals, memory, sample preparation

ABSTRACT

Transition metal ions (Fe, Mn, Cu, Zn) are essential for healthy brain function, but altered concentration, distribution, or chemical form of the metal ions has been implicated in numerous brain pathologies. Currently, it is not possible to image the cellular or sub-cellular distribution of metal ions *in vivo* and therefore, studying brain-metal homeostasis largely relies on *ex vivo in situ* elemental mapping. Sample preparation methods that accurately preserve the *in vivo* elemental distribution are essential if one wishes to translate the knowledge of elemental distributions measured *ex vivo* toward increased understanding of chemical and physiological pathways of brain disease. The choice of sample preparation is particularly important for metal ions that exist in a labile or mobile form, for which the *in vivo* distribution could be easily distorted by inappropriate sample preparation. One of the most widely studied brain structures, the hippocampus, contains a large pool of labile and mobile Zn. Herein, we describe how sucrose cryoprotection, the gold standard method of preparing tissues for immuno-histochemistry or immuno-fluorescence, which is also often used as a sample preparation method for elemental mapping studies, drastically alters hippocampal Zn distribution. Based on the results of this study, in combination with a comparison against the strong body of published literature that has used either rapid plunge freezing of brain tissue, or sucrose cryo-protection, we strongly urge investigators in the future to cease using sucrose cryoprotection as a method of sample preparation for elemental mapping, especially if Zn is an analyte of interest.

INTRODUCTION

Zn is the second most abundant trace element in the brain, and essential for brain function. The average Zn concentration in a mouse or rat brain is on the order of several hundred µM.[1-5] Interestingly, there is a subset of glutamatergic neurons found within layers III and V of the cortex, olfactory bulb, striatum, and hippocampus, which, although contributing to less than 5 % of total brain Zn, contain substantially elevated local Zn concentration (reported to approach 1 mM).[3, 6] The chemical form of Zn contained within Zn enriched neurons is mostly labile (*i.e.*, complexed to readily exchangeable ligands) and mobile (*i.e.*, is released into the synaptic cleft during neuronal excitation).[6-8] The labile and mobile nature of this Zn pool enables detection using classical histochemical stains for labile metal ions: *e.g.*, Timm's stain and Danscher methods;[7, 9, 10] or the more recently developed Zn sensitive fluorescence sensors; TSQ, Newport Green. FuraZin, FluoZin, Znpyr, and ZnAF, as reviewed elsewhere.[11, 12] Histochemical methods and fluorescence sensors have been immensely useful when applied to *in vitro* cell culture or organotypical tissue slice models.[11, 13] In addition, perfusion of living animals with histochemical reagents enables the *in vivo* labile Zn pool to be visualised in brain tissue generated from animal models.[7, 9-11] There are however, limitations to the above methods:[11, 14-17] specificity issues may occur with cross reactivity of stains and sensors with other divalent metal ions (though designed to be minimal), sequestered or non-labile forms of Zn are not detected, the methods do not typically differentiate between multiple chemical forms of labile Zn, and disease states that alter cell membrane permeability may affect stain penetration though cells and tissues. As a hypothetical example, two samples with identical chemical form, amount, and distribution of Zn may produce two different patterns of staining if there are differences in the ability of the stain or sensor to permeate the tissue.

Spectroscopic methods capable of direct Zn detection do not suffer the limitations of histochemical stains or fluorescence probes described above, but in general direct spectroscopic detection does not offer the same level of chemical specificity. Elemental mapping techniques such as laser ablation inductively coupled plasma mass spectrometry (LA-ICP-MS), X-ray fluorescence microscopy (XFM), or proton-induced X-ray emission spectrometry (PIXE) have therefore, been widely adopted to image total Zn distribution within the brain. Multiple investigators have applied elemental mapping to characterise the baseline Zn distribution in the healthy rodent brain,[18-30] during brain development and ageing,[31-33] after injury such us stroke,[28, 34-36] brain trauma,[37-39] following potential Mn toxicity,[40, 41] and in disease states, such as epilepsy,[42-44] Alzheimer's disease and dementia,[45-52] and Parkinson's disease.[28, 53-55]

The fact that a portion of brain Zn is coordinatively labile and also mobile demands that appropriate sample preparation protocols are employed to adequately preserve the *in vivo* Zn distribution. If inappropriate methods are used there is substantial risk to disturb and alter the endogenous Zn distribution, which is already known from extensive histochemical studies.[7, 9-11] Further, past studies have shown that chemical fixation methods (*e.g.*, formalin fixation) can leach or redistribute metal ions from brain tissue, and trace metal ion contamination in fixation media can artificially increase metal ion content.[56-59] It is thus recommended that chemical fixation of tissues should be avoided for elemental mapping. Indeed, one of the major analytical advantages of XFM (or PIXE) and LA-ICP-MS is that they offer a direct reagent- and stain-free method for elemental detection. It is therefore perplexing that many studies still choose to prepare biological tissues using traditional chemical fixation and cryo-protection methods that were developed in an era before these more subtle properties of labile and mobile metals was widely appreciated. Specifically, sucrose cryo-protection (SCP) remains an accepted tissue preparation method for elemental mapping in pre-clinical studies of rodent brain tissue.

Tissue freezing is required to maintain optimum protein antigenicity during tissue storage, and SCP is arguably the gold-standard choice of sample preparation in the field of immuno-histochemistry (IHC) and immuno-fluorescence (IF). SCP is widely used for IHC and IF, as it provides excellent preservation of cell structures and maintains protein antigenicity, while minimising formation of ice-crystals during tissue freezing. The wide-spread use of SCP in the IHC and IF fields, and the growth of multimodal imaging studies (i.e., combined elemental mapping with IF or IHC),[60] may explain why many elemental mapping studies have adopted SCP for sample preparation without further scrutiny. Although the broader effects of chemical fixation on elemental distribution have been well-characterised,[56-59] to our knowledge no study has specifically reported the effects of SCP on elemental distribution (specifically Zn distribution) within the hippocampus.

The hippocampus has a highly organised structure, is critical to spatial learning and memory, and is enriched in labile Zn.[6-8, 19, 61] Labile Zn is known to modulate hippocampal memory function, and disturbed hippocampal Zn is associated with brain pathology, including memory loss and cognitive decline.[6, 8, 46, 61-64] The distribution of labile Zn within the hippocampus, as determined by classical histochemical methods, is well-characterised, and has a highly reproducible localisation to specific hippocampal sub-regions.[7, 8, 11] We have performed a search of the literature, which revealed 30 studies reporting elemental maps of hippocampal Zn distribution; 23/30 use rapid plunge freezing (RPF) in either liquid nitrogen or liquid nitrogen cooled isopentane, 6/30 use SCP (i.e., 20 %), and in 1/30 the sample preparation method was undefined.[19-24, 29-33, 36, 39-44, 46, 47, 49-52, 54, 55, 65-68] In all studies where elemental mapping was performed on brain tissue prepared via RPF, highly reproducible hippocampal Zn distribution was reported (regardless of the animal model used), and the distribution strongly resembles the distribution of labile Zn shown in histochemical studies. In studies reporting elemental distributions from tissue prepared via SCP, substantial variation in the Zn distribution can be observed. In studies where SCP tissues show a drastically different distribution to that observed in tissue prepared via RPF, there is a visible trend in the pattern of redistribution. The characteristic features of hippocampal Zn distribution that are always observed in tissues prepared by RPF, which are not always observed in tissues prepared by SCP, are:

1. *In tissue prepared via RPF the "mossy fibres" are the most Zn enriched hippocampal sub-region, containing Zn levels at least double that of other sub-regions of the hippocampus, and the surrounding cortical and white matter structures (e.g., alveus, corpus callosum).*
2. *There is well defined contrast between the Zn content of the CA1 stratum radiatum (relatively higher Zn content) and the dentate gyrus molecular layer (relatively lower Zn content), in tissues prepared via RPF.*
3. *There is localised Zn enrichment within the pyramidal neuron layer and dentate gyrus granule neuron layer, in tissues prepared via RPF (this will only be observed if images are collected with sufficient spatial resolution to resolve these cell layers, which are only 2-3 cells wide)*
4. *Tissues prepared via RPF do not display Zn enrichment or a "Zn halo" at the interface of the hippocampus and the white matter structures that encase the hippocampus.*

There could be a number of experimental factors that result in the variation of Zn distribution that is observed in past studies that have used SCP, such as variation in animal strain, animal age, and tissue section thickness. The aim of our current study is not to discredit or disparage past work, however, it is our view that a detailed understanding of the nature of the hippocampal Zn redistribution that occurs in SCP tissues is critically needed to aid future experimental design and to avoid misinterpretations of experimental artifacts that may arise from the use of SCP in this context.

Herein, we present a side-by-side intra-animal comparison of hippocampal Zn distribution in brain hemispheres from mice and rats (in duplicate), which were prepared through either rapid plunge freezing in liquid nitrogen cooled iso-pentane (RPF, left hemisphere) or through sucrose cryo-protection (SCP, right hemisphere). We have previously shown that differences in Zn content and distribution are not observed between the left and right hemispheres in naïve brain tissue prepared via RPF.[36] As such, our results support that a dramatic redistribution of Zn occurs during SCP. The pattern of Zn redistribution we observed can account for the variation in Zn distribution observed in the literature when comparing tissues prepared via RPF or SCP. Based on our results we strongly urge that the use of SCP be abandoned as an accepted sample preparation method in any future XFM or LA-ICP-MS studies, especially those that aim to investigate disease mechanisms through analysis of hippocampal Zn.

METHODS

A rationale for our experimental design is provided in Supporting Information.

Animals

This study has compared Zn distribution in the hippocampus of two mice (senescence accelerated murine prone – strain 8, SAMP8) and two outbred rats (Sprague Dawley). The mice were 12 week old males, and the rats were 6 week old males. All animals were housed in standard cages in a temperature controlled (21 °C) colony room on a 12/12 h light/dark cycle with standard rodent maintenance chow and water available ad libitum. The rat experiment was approved by the University of Saskatchewan's Animal Research Ethics Board, and adhered to the Canadian Council on Animal Care guidelines for humane animal use. All experimental procedures for the mice experiment were conducted in accordance with Curtin University Animal Ethics Guidelines.

Tissue Collection and Sample preparation

Rat tissue was prepared at the University of Saskatchewan and mouse tissue was prepared at Curtin University. Sample preparation procedures were identical between the rat and mouse brains, and similar to previously described.[69] Specifically, for this study: animals were anaesthetized with isoflurane, and humanely sacrificed through cervical dislocation and decapitation. The brain was immediately removed from the skull, and cut into two equal sagittal hemispheres. The left hemisphere was immediately plunge frozen in liquid-nitrogen cooled isopentane, i.e., rapid plunge freezing (RPF). The right hemisphere was fixed overnight in 4 % buffered formalin, before being transferred into graduated sucrose cryo-protection solutions. After sucrose cryo-protection, the brain hemisphere was flash frozen in liquid nitrogen. Tissue sections for XFM elemental mapping were cut with a cryo-microtome at -18 ˚C at a thickness of 10-μm (coronal plane), and at a brain location of -3.3 to -2.7 mm relative to Bregma in rats, and -1.3 to -2.2 mm relative to Bregma in mice. Mouse tissue sections were melted onto silicon nitride substrate, 10x10 mm^2 silicon frame, 200 μm thick, 5x5 mm^2 silicon nitride membrane 1 μm thick, (Melbourne Centre for Nanofabrication, MCN), for imaging at the X-ray fluorescence microscopy beamline at the Australian Synchrotron. Rat tissue sections were cut onto 200 μm-thick metal free Thermanox plastic substrate (Thermo Scientific), for elemental mapping at beamline 10-2 at the Stanford Synchrotron Radiation Light Source. For both mouse and rat brains, serial tissue sections were cut and mounted on glass microscope slides for H&E histology (also cut at 10-μm-thick). Tissue sections for histology were cut at a location within 200 μm of the sections analysed by XFM.

Synchrotron XFM Elemental Mapping of Hippocampal Zn Distribution

Elemental mapping of mouse hippocampal tissue was performed at the X-ray fluorescence microscopy beamline at the Australian Synchrotron, using a monochromatic incident beam of 15.8 keV, focused to a 2 μm (2-sigma) spot with a Kirkpatrick–Baez mirror pair. Experimental parameters were identical to those previously reported.[65, 67] Specifically, and as previously reported, data was collected with the sample orientated normal to the incident beam and with the Maia detector positioned in backscatter geometry, with the sample raster scanned through the beam using an effective dwell time of 0.1 ms and an effective step (pixel) size of 1 μm. Elemental foils (MicroMatter Technologies Inc., Canada), were scanned in the same geometry and used as references for elemental quantification, as previously reported. Elemental maps were reconstructed from the full X-ray emission spectra with GeoPIXE v6.6j. (CSIRO, Australia), which uses a linear transformation matrix for spectral deconvolution.[70, 71] Quantitative data were extracted as tiff files of quantitative per-pixel elemental area density in ng cm^{-2}, which were then imported into ImageJ v1.48, as described previously. All regions of interest, and the average elemental areal density, were calculated using ImageJ. Tissue samples were considered as "semi-thin" with respect to self-absorption, as demonstrated by other authors.[73]

Zn distribution in the rat hippocampus sections were collected using XFM at the Stanford Synchrotron Radiation Lightsource (SSRL) experimental station 10-2 (http://www-ssrl.slac.stanford.edu/beamlines/bl10-2/). The energy of the incident X-ray beam was 13.5 keV, and the beamline configuration was as previously reported.[18] A pin hole aperture (50 μm) was positioned to yield an X-ray spot size of approximately 50 μm at the sample plane, which was mounted at 45° to the incident beam. The sample was raster scanned through the beam, with an exposure time of 100 ms per 30 μm step. X-ray emission spectra were recorded with a 4-element Vortex® silicon drift detector at 90° to the incident beam. Zn elemental maps were obtained as single channel data (not fitted

MCAs). Elemental maps were quantified using Zn reference foils, National Institute of Standards and Technology (NIST) reference standard (SRM #19176), as previously described.[18] SSRL data was processed using the MicroAnalysis Toolkit (version 1.50).[72]

H&E Histology

To demonstrate the anatomical sub-regions within the hippocampus, routine haematoxylin and eosin (H&E) staining was performed, using a standard protocol. Microscopy images of the H&E stained tissue were acquired at 4x magnification using an Olympus Bx51 microscope with an Olympus dp70 camera, and cellSens standard software.

Data Analysis

Elemental maps of Zn distribution were prepared using Image J software, with the min and max colour intensity set to the same value for the left (RPF) and right (SCP) brain tissue. Due to the low number of replicates, quantitative statistical analysis was not undertaken; rather, qualitative comparison of Zn distribution is reported only.

RESULTS & DISCUSSION

Zn is depleted from specific hippocampus sub-regions during sucrose cryo-protection in mice

Comparison of the hippocampal Zn distribution in mice, in tissue prepared via RPF or SCP is shown in Figure 1 (mouse replicate 1) and Figure 2 (mouse replicate 2). The major anatomical features of the hippocampus have been outlined in the H&E histological image presented in Figure 1A. It is well established that the hippocampal mossy fibres are highly enriched in labile Zn (regions a_1 and a_2),[7, 10, 74] and this region can be seen to contain the highest concentration of Zn in both RPF and SCP tissues. Although the mossy fibres do appear enriched in Zn in the SCP tissue, it is clear that the Zn levels are reduced in mossy fibre region of SCP tissue relative to RPF tissue (*i.e.*, comparison of Figure 1 panels B *vs*. C, D *vs*. F, H *vs*. I, and comparison of Figure 2 panels A *vs*. B, C *vs*. E, G *vs*. H).

The pyramidal cell layer (region *e*), and dentate gyrus granule cell layer (region *b*) appear relatively Zn enriched in RPF tissue, but this observation is in contrast with the apparently depleted Zn content, relative to surrounding neuropil, in SCP-treated tissue, *e.g.* comparison of Figure 1 panels B *vs*. C, D *vs*. F and E *vs*. G, and comparison of Figure 2 panels A *vs*. B, C *vs*. E, D, *vs*. F. Interestingly, traditional histochemical methods that reveal labile Zn do not routinely show a labile Zn pool within pyramidal or granule cell neurons,[7, 10, 74] which could indicate that this intra-cellular Zn is predominantly protein bound and non-labile. The difference in Zn distribution within the pyramidal and granule cell layers between RPF and SCP tissues in our data however, suggests that a component of the intra-cellular Zn pool is at least mobile, if not labile. It is possible that histochemical methods do not detect labile intra-cellular Zn within neurons as the stains do not penetrate the cell membranes of intact, healthy cells in living animals. Looking at the published *in vitro* literature, where cell permeability and uptake mechanisms differ from the *in vivo* state, labile Zn is detected within neurons in cell culture.[75] Taken together, our data and the published literature suggest there is a mobile pool of Zn within neuron cell bodies, which is not normally detected by histochemical stains, and this pool of Zn can be lost or redistributed during SCP.

The CA1 stratum radiatum (region *d*) is known to be enriched in labile Zn,[7, 10, 74] albeit not to the same extent as the mossy fibres. Conversely, very little labile Zn is observed in the dentate gyrus molecular layer (region *c*) that is located ventral to the CA1 stratum radiatum and ventral to the hippocampal fissure.[7, 10, 74] On the basis of the above, histochemical staining for labile Zn shows well-defined contrast in staining between the CA1 stratum radiatum and the adjacent dentate gyrus molecular layer.[7, 10, 74] This staining pattern is reproduced in images from our current study, for tissues prepared via RPF *i.e.*, increased Zn levels are observed in the CA1 stratum radiatum relative to the dentate gyrus molecular layer (Figure 1 panels B, E and Figure 2 panels A, D). The Zn appears to have been lost from the CA1 stratum radiatum in SCP tissue however, resulting in an apparent uniform distribution of Zn content across the CA1 stratum radiatum and dentate gyrus molecular layer (Figure 1 panels C, G, and Figure 2 panels B, F). The variation in Zn contrast across the CA1 stratum radiatum and dentate gyrus molecular layer between RPF and SCP tissues can also be seen in line plots of Zn areal density across these regions (Figure 3).

Zn is locally enriched in white matter that surrounds the hippocampus as a consequence of sucrose cryo-protection, in mice

The results presented thus far indicate that SCP results in substantial mobilisation of Zn from hippocampal regions naturally enriched in labile Zn, which is not unexpected. The question that remains is whether the mobilised Zn is leached completely from the brain tissue, or if some of this labile pool instead binds to a different tissue region. Endogenous Zn content within white matter is naturally low,[2, 3] but amino acid residues in white matter proteins (*e.g.*, histidine residues in myelin basic protein, which are potent coordinators of Zn ions[76]) or the phospholipid head groups, could potentially compete for, and coordinate, Zn if exposed to a labile Zn pool that has been mobilized from its source location in the tissue. Under normal brain physiological conditions the white matter is not exposed to a mobile, labile Zn pool,[2, 3, 6, 7] however, this could occur during SCP when Zn ions are mobilized from the hippocampus. As can be seen in Figure 1 panels C and I, and Figure 2 panels B and H, there is a substantial relative increase in Zn content at the periphery of the hippocampus (referred to as a Zn "halo"). The hippocampus is encased in white matter, bounded specifically the alveus, cingulum, and corpus callosum, and strong Zn enrichment is observed at the interface of the hippocampus and the white matter structures in SCP

treated tissue (Figure 3). The Zn "halo" surrounding the hippocampus is not observed in RPF tissue (Figure 1 B, H, Figure 2 A, G, and Figure 3).

The effect of sucrose cryo-protection on Zn distribution in the rat hippocampus is similar to that observed in mice

Due to limited availability of synchrotron time, analyses of mice and rat tissue were performed at different synchrotron facilities. Mouse tissues were analysed at the XFM beamline of the Australian Synchrotron (1 µm pixel resolution, with KB mirrors), while rat tissues were analysed at beamline 10-2 at SSRL (50 µm spatial resolution with a pin-hole aperture). Due to the more-coarse spatial resolution for the analysis of rat tissue, qualitative assessment of Zn distribution is limited to larger brain structures (*i.e.*, individual cell layers could not be resolved). Nonetheless, in duplicate measurements, there is a clear redistribution of Zn as a consequence of SCP preparation (relative to RPF), and this mirrors the findings observed in mice. Specifically, there is a drastic reduction of Zn in the mossy fibre regions of SCP tissue in rats (regions a_1 and a_2), while the white matter structures that border the hippocampus (regions f_1 and f_2) display a substantive increase in Zn areal density (Figure 4 and Figure 5). In addition, the contrast in Zn levels between the dentate gyrus molecular layer and the CA1 stratum radiatum is not apparent in SCP-prepared rat tissue, consistent with the results demonstrated in mice (Figure 4 and Figure 5).

CONCLUSIONS AND RECOMMENDATIONS

The results of this study, when considered alongside the data published in the literature, strongly support that sucrose cryo-protection results in substantial Zn redistribution in the hippocampus. It is impossible to determine if the redistribution will occur in all experimental cases, or if it will occur to the same magnitude in all cases, but it is clear that SCP is not well suited to preserve the *in vivo* hippocampal Zn distribution. The results of this study also indicate that due to the redistribution phenomena, samples prepared identically, may not experience identical magnitude of redistribution. For example, disease processes or brain injury often affect cell membrane permeability and result in varying levels of inflammation or metabolic alterations that can drastically affect protein synthesis (*i.e.*, affect availability of Zn binding sites). Therefore, in a hypothetical scenario, the *in vivo* hippocampal Zn distribution could be identical between two experimental groups, but, unless protein expression and cell membrane permeability are also identical between the experimental groups, the use of SCP during sample preparation may induce differences in Zn distribution that is associated with the differential mobility of Zn across cell membranes and differential opportunities for Zn binding throughout the tissue. We strongly urge investigators in the field to move away from the use of sucrose cryo-protection in animal tissues for elemental mapping, especially if the tissue is known to contain a substantive proportion of labile or mobile metal ions.

AUTHOR CONTRIBUTIONS

MJP and MJH formulated scientific ideas for manuscript. MJH and MJP were major writers and editors of manuscript. MJH coordinated collaboration between other co-authors.

AH (PhD student of MJH) and JR collected and analysed Australian Synchrotron data.

SW, IJP, GNG, and MJH collected and analysed SSRL data.

VL prepared murine mouse samples, including perfusion, using SAMP8 animal model maintained by RT and JCLM.

MJH and PGP prepared rat tissue samples.

MEK provided expertise on brain neuroanatomy in mice and rat models.

All authors contributed to editing manuscript.

REFERENCES

1.   Kofod, B., Iron, copper, and zinc in rat brain. *Eur. J. Pharmacol.* **1970,** *13* (1), 40-45.
2.   Takeda, A., Movement of zinc and its functional significance in the brain. *Brain Res. Rev.* **2000,** *34* (3), 137-148.
3.   Frederickson, C. J.; Klitenick, M. A.; Manton, W. I.; Kirkpatrick, J. B., Cytoarchitectonic distribution of zinc in the hippocampus of man and the rat. *Brain Res.* **1983,** *273* (2), 335-339.
4.   Markesbery, W. R.; Ehmann, W. D.; Alauddin, M.; Hossain, T., Brain trace element concentrations in aging. *Neurobiol. Aging* **1984,** *5* (1), 19-28.
5.   Takeda, A.; Takefuta, S.; Okada, S.; Oku, N., Relationship between brain zinc and transient learning impairment of adult rats fed zinc-deficient diet. *Brain Res.* **2000,** *859* (2), 352-357.
6.   Frederickson, C. J.; Suh, S. W.; Silva, D.; Frederickson, C. J.; Thompson, R. B., Importance of Zn in the central nervous system: the Zinc-containing neuron. *The Journal of Nutrition* **2000,** *130*, 1471-1483.
7.   Frederickson, C.; Rampy, B.; Reamy-Rampy, S.; Howell, G., Distribution of histochemically reactive zinc in the forebrain of the rat. *J. Chem. Neuroanat.* **1992,** *5* (6), 521-530.
8.   Frederickson, C. J.; Koh, J.-Y.; Bush, A. I., The neurobiology of zinc in health and disease. *Nature Reviews Neuroscience* **2005,** *6* (6), 449-462.
9.   Danscher, G., Histochemical demonstration of heavy metals. *Histochemistry* **1981,** *71* (1), 1-16.
10.   Danscher, G.; Zimmer, J., An improved Timm sulphide silver method for light and electron microscopic localization of heavy metals in biological tissues. *Histochem. Cell Biol.* **1978,** *55* (1), 27-40.
11.   Frederickson, C. J.; Kasarskis, E.; Ringo, D.; Frederickson, R., A quinoline fluorescence method for visualizing and assaying the histochemically reactive zinc (bouton zinc) in the brain. *J. Neurosci. Methods* **1987,** *20* (2), 91-103.
12.   Hyman, L. M.; Franz, K. J., Probing oxidative stress: Small molecule fluorescent sensors of metal ions, reactive oxygen species, and thiols. *Coord. Chem. Rev.* **2012,** *256* (19), 2333-2356.
13.   Nydegger, I.; Rumschik, S. M.; Zhao, J.; Kay, A. R., Evidence for an extracellular zinc-veneer in rodent brains from experiments with Zn-ionophores and ZnT3 knockouts. *ACS Chem. Neurosci.* **2012,** *3* (10), 761-766.
14.   Thompson, R.; Peterson, D.; Mahoney, W.; Cramer, M.; Maliwal, B. P.; Suh, S. W.; Frederickson, C.; Fierke, C.; Herman, P., Fluorescent zinc indicators for neurobiology. *J. Neurosci. Methods* **2002,** *118* (1), 63-75.
15.   Kay, A. R., Imaging synaptic zinc: promises and perils. *Trends Neurosci.* **2006,** *29* (4), 200-206.
16.   Nowakowski, A. B.; Petering, D. H., Reactions of the fluorescent sensor, zinquin, with the zinc-proteome: Adduct formation and ligand substitution. *Inorg. Chem.* **2011,** *50* (20), 10124-10133.
17.   Lenglet, W.; Bos, A.; vd Stap, C.; Vis, R.; Delhez, H.; vd Hamer, C., Discrepancies between histological and physical methods for trace element mapping in the rat brain. *Histochemistry* **1984,** *81* (3), 305-309.

18.	Alaverdashvili, M.; Hackett, M. J.; Pickering, I. J.; Paterson, P. G., Laminar-specific distribution of zinc: Evidence for presence of layer IV in forelimb motor cortex in the rat. *NeuroImage* **2014,** *103*, 502-510.

19.	Linkous, D. H.; Flinn, J. M.; Koh, J. Y.; Lanzirotti, A.; Bertsch, P. M.; Jones, B. F.; Giblin, L. J.; Frederickson, C. J., Evidence that the ZNT3 protein controls the total amount of elemental zinc in synaptic vesicles. *J. Histochem. Cytochem.* **2008,** *56* (1), 3-6.

20.	Paul, B.; Hare, D. J.; Bishop, D. P.; Paton, C.; Cole, N.; Niedwiecki, M. M.; Andreozzi, E.; Vais, A.; Billings, J. L.; Bray, L., Visualising mouse neuroanatomy and function by metal distribution using laser ablation-inductively coupled plasma-mass spectrometry imaging. *Chemical Science* **2015,** *6* (10), 5383-5393.

21.	Hare, D. J.; Lee, J. K.; Beavis, A. D.; van Gramberg, A.; George, J.; Adlard, P. A.; Finkelstein, D. I.; Doble, P. A., Three-dimensional atlas of iron, copper, and zinc in the mouse cerebrum and brainstem. *Anal. Chem.* **2012,** *84* (9), 3990-3997.

22.	HM Ali, M.; Rakib, F.; Nischwitz, V.; Ullah, E.; Mall, R.; Shraim, A. M.; Ahmad, M.; Ghouri, Z. K.; McNaughton, D.; Küppers, S., Application of FTIR and LA-ICPMS spectroscopies as a possible approach for biochemical analyses of different rat brain regions. *Applied Sciences* **2018,** *8* (12), 2436.

23.	Urgast, D. S.; Hill, S.; Kwun, I.-S.; Beattie, J. H.; Goenaga-Infante, H.; Feldmann, J., Zinc isotope ratio imaging of rat brain thin sections from stable isotope tracer studies by LA-MC-ICP-MS. *Metallomics* **2012,** *4* (10), 1057-1063.

24.	Hare, D. J.; Lear, J.; Bishop, D.; Beavis, A.; Doble, P. A., Protocol for production of matrix-matched brain tissue standards for imaging by laser ablation-inductively coupled plasma-mass spectrometry. *Analytical Methods* **2013,** *5* (8), 1915-1921.

25.	Kemp, K.; Danscher, G., Multi-element analysis of the rat hippocampus by proton induced X-ray emission spectroscopy (phosphorus, sulphur, chlorine, potassium, calcium, iron, zinc, copper, lead, bromine, and rubidium). *Histochemistry* **1979,** *59* (3), 167-176.

26.	Lear, J.; Hare, D. J.; Fryer, F.; Adlard, P. A.; Finkelstein, D. I.; Doble, P. A., High-resolution elemental bioimaging of Ca, Mn, Fe, Co, Cu, and Zn employing LA-ICP-MS and hydrogen reaction gas. *Anal. Chem.* **2012,** *84* (15), 6707-6714.

27.	Jackson, B.; Harper, S.; Smith, L.; Flinn, J., Elemental mapping and quantitative analysis of Cu, Zn, and Fe in rat brain sections by laser ablation ICP-MS. *Anal. Bioanal. Chem.* **2006,** *384* (4), 951-957.

28.	Becker, J. S.; Matusch, A.; Becker, J. S.; Wu, B.; Palm, C.; Becker, A. J.; Salber, D., Mass spectrometric imaging (MSI) of metals using advanced BrainMet techniques for biomedical research. *Int. J. Mass spectrom.* **2011,** *307* (1), 3-15.

29.	Wu, B.; Becker, J. S., Bioimaging of metals in rat brain hippocampus by laser microdissection inductively coupled plasma mass spectrometry (LMD-ICP-MS) using high-efficiency laser ablation chambers. *Int. J. Mass spectrom.* **2012,** *323-324*, 34-40.

30.	Pushie, M. J.; Pickering, I. J.; Martin, G. R.; Tsutsui, S.; Jirik, F. R.; George, G. N., Prion protein expression level alters regional copper, iron and zinc content in the mouse brain. *Metallomics* **2011,** *3* (2), 206-214.

31.	Fimognari, N.; Hollings, A.; Lam, V.; Tidy, R. J.; Kewish, C. M.; Albrecht, M. A.; Takechi, R.; Mamo, J. C. L.; Hackett, M. J., Biospectroscopic Imaging Provides Evidence of Hippocampal Zn Deficiency and Decreased Lipid Unsaturation in an Accelerated Aging Mouse Model. *ACS Chem. Neurosci.* **2018,** *9* (11), 2774-2785.

32.	Chwiej, J.; Palczynska, M.; Skoczen, A.; Janeczko, K.; Cieslak, J.; Simon, R.; Setkowicz, Z., Elemental changes of hippocampal formation occurring during postnatal brain development. *J. Trace Elem. Med Biol.* **2018,** *49*, 1-7.

33.	Ashraf, A.; Michaelides, C.; Walker, T. A.; Ekonomou, A.; Suessmilch, M.; Sriskanthanathan, A.; Abraha, S.; Parkes, A.; Parkes, H. G.; Geraki, K., Regional distributions of iron, copper and zinc and their relationships with glia in a normal aging mouse model. *Front. Aging Neurosci.* **2019,** *11*.

34.	Caine, S.; Hackett, M. J.; Hou, H.; Kumar, S.; Maley, J.; Ivanishvili, Z.; Suen, B.; Szmigielski, A.; Jiang, Z.; Sylvain, N. J.; Nichol, H.; Kelly, M. E., A novel multi-modal platform to image molecular and elemental alterations in ischemic stroke. *Neurobiol. Dis.* **2016,** *91*, 132-142.

35.	Pushie, M. J.; Crawford, A. M.; Sylvain, N. J.; Hou, H.; Hackett, M. J.; George, G. N.; Kelly, M. E., Revealing the Penumbra through Imaging Elemental Markers of Cellular Metabolism in an Ischemic Stroke Model. *ACS Chem. Neurosci.* **2018,** (9), 886-893.

36.	Silasi, G.; Klahr, A. C.; Hackett, M. J.; Auriat, A. M.; Nichol, H.; Colbourne, F., Prolonged therapeutic hypothermia does not adversely impact neuroplasticity after global ischemia in rats. *J. Cereb. Blood Flow Metab.* **2012,** *32* (8), 1525-1534.

37.   Hartnell, D.; Gillespie-Jones, K.; Ciornei, C.; Hollings, A.; Thomas, A.; Harrild, E.; Reinhardt, J.; Paterson, D. J.; Alwis, D.; Rajan, R., Characterisation of Ionic and Lipid Gradients within Corpus Callosum White Matter after Diffuse Traumatic Brain Injury in the Rat. *ACS Chem. Neurosci.* **2019**.

38.   Chwiej, J.; Sarapata, A.; Janeczko, K.; Stegowski, Z.; Appel, K.; Setkowicz, Z., X-ray fluorescence analysis of long-term changes in the levels and distributions of trace elements in the rat brain following mechanical injury. *JBIC Journal of Biological Inorganic Chemistry* **2011**, *16* (2), 275-283.

39.   Portbury, S. D.; Hare, D. J.; Sgambelloni, C.; Finkelstein, D. I.; Adlard, P. A., A time-course analysis of changes in cerebral metal levels following a controlled cortical impact. *Metallomics* **2016**, *8* (2), 193-200.

40.   Daoust, A.; Barbier, E. L.; Bohic, S., Manganese enhanced MRI in rat hippocampus: A correlative study with synchrotron X-ray microprobe. *NeuroImage* **2013**, *64*, 10-18.

41.   Robison, G.; Zakharova, T.; Fu, S.; Jiang, W.; Fulper, R.; Barrea, R.; Zheng, W.; Pushkar, Y., X-ray fluorescence imaging of the hippocampal formation after manganese exposure. *Metallomics* **2013**, *5* (11), 1554-1565.

42.   Chwiej, J.; Dulinska, J.; Janeczko, K.; Appel, K.; Setkowicz, Z., Variations in elemental compositions of rat hippocampal formation between acute and latent phases of pilocarpine-induced epilepsy: an X-ray fluorescence microscopy study. *JBIC Journal of Biological Inorganic Chemistry* **2012**, *17* (5), 731-739.

43.   Chwiej, J.; Kutorasinska, J.; Janeczko, K.; Gzielo-Jurek, K.; Uram, L.; Appel, K.; Simon, R.; Setkowicz, Z., Progress of elemental anomalies of hippocampal formation in the pilocarpine model of temporal lobe epilepsy: an X-ray fluorescence microscopy study. *Anal. Bioanal. Chem.* **2012**, *404* (10), 3071-3080.

44.   Chwiej, J.; Winiarski, W.; Ciarach, M.; Janeczko, K.; Lankosz, M.; Rickers, K.; Setkowicz, Z., The role of trace elements in the pathogenesis and progress of pilocarpine-induced epileptic seizures. *JBIC Journal of Biological Inorganic Chemistry* **2008**, *13* (8), 1267-1274.

45.   Summers, K. L.; Fimognari, N.; Hollings, A.; Kiernan, M.; Lam, V.; Tidy, R. J.; Paterson, D.; Tobin, M. J.; Takechi, R.; George, G. N.; Pickering, I. J.; Mamo, J. C.; Harris, H. H.; Hackett, M. J., A Multimodal Spectroscopic Imaging Method To Characterize the Metal and Macromolecular Content of Proteinaceous Aggregates ("Amyloid Plaques"). *Biochemistry* **2017**, *56* (32), 4107-4116.

46.   Adlard, P. A.; Parncutt, J.; Lal, V.; James, S.; Hare, D.; Doble, P.; Finkelstein, D. I.; Bush, A. I., Metal chaperones prevent zinc-mediated cognitive decline. *Neurobiol. Dis.* **2015**, *81*, 196-202.

47.   James, S. A.; Churches, Q. I.; de Jonge, M. D.; Birchall, I. E.; Streltsov, V.; McColl, G.; Adlard, P. A.; Hare, D. J., Iron, Copper, and Zinc Concentration in Aβ Plaques in the APP/PS1 Mouse Model of Alzheimer's Disease Correlates with Metal Levels in the Surrounding Neuropil. *ACS Chem. Neurosci.* **2017**, *8*, 629-637.

48.   Miller, L. M.; Wang, Q.; Telivala, T. P.; Smith, R. J.; Lanzirotti, A.; Miklossy, J., Synchrotron-based infrared and X-ray imaging shows focalized accumulation of Cu and Zn co-localized with beta-amyloid deposits in Alzheimer's disease. *J. Struct. Biol.* **2006**, *155* (1), 30-37.

49.   Leskovjan, A. C.; Kretlow, A.; Lanzirotti, A.; Barrea, R.; Vogt, S.; Miller, L. M., Increased brain iron coincides with early plaque formation in a mouse model of Alzheimer's disease. *NeuroImage* **2011**, *55* (1), 32-38.

50.   Wang, H.-J.; Wang, M.; Wang, B.; Meng, X.-Y.; Wang, Y.; Li, M.; Feng, W.-Y.; Zhao, Y.-L.; Chai, Z.-F., Quantitative imaging of element spatial distribution in the brain section of a mouse model of Alzheimer's disease using synchrotron radiation X-ray fluorescence analysis. *J. Anal. At. Spectrom.* **2010**, *25* (3), 328-333.

51.   Wang, H.; Wang, M.; Wang, B.; Li, M.; Chen, H.; Yu, X.; Zhao, Y.; Feng, W.; Chai, Z., The distribution profile and oxidation states of biometals in APP transgenic mouse brain: dyshomeostasis with age and as a function of the development of Alzheimer's disease. *Metallomics* **2012**, *4* (3), 289-296.

52.   Hackett, M. J.; Hollings, A.; Majimbi, M.; Brook, E.; Cochran, B.; Giles, C.; Lam, V.; Nesbit, M.; Rye, K.-A.; Mamo, J. C., Multimodal Imaging Analyses of Brain Hippocampal Formation Reveal Reduced Cu and Lipid Content and Increased Lactate Content in Non-Insulin-Dependent Diabetic Mice. *ACS Chem. Neurosci.* **2019**, *10* (5), 2533-2540.

53.   Carmona, A.; Roudeau, S.; Perrin, L.; Carcenac, C.; Vantelon, D.; Savasta, M.; Ortega, R., Mapping Chemical Elements and Iron Oxidation States in the Substantia Nigra of 6-Hydroxydopamine Lesioned Rats Using Correlative Immunohistochemistry With Proton and Synchrotron Micro-Analysis. *Front. Neurosci.* **2019**, *13*, 1014.

54.   Hare, D. J.; George, J. L.; Grimm, R.; Wilkins, S.; Adlard, P. A.; Cherny, R. A.; Bush, A. I.; Finkelstein, D. I.; Doble, P., Three-dimensional elemental bio-imaging of Fe, Zn, Cu, Mn and P in a 6-hydroxydopamine lesioned mouse brain. *Metallomics* **2010**, *2* (11), 745-753.

55.   Matusch, A.; Depboylu, C.; Palm, C.; Wu, B.; Höglinger, G. U.; Schäfer, M. K.-H.; Becker, J. S., Cerebral bioimaging of Cu, Fe, Zn, and Mn in the MPTP mouse model of Parkinson's disease using laser ablation inductively coupled plasma mass spectrometry (LA-ICP-MS). *J. Am. Soc. Mass Spectrom.* **2010,** *21* (1), 161-171.

56.   Hackett, M. J.; McQuillan, J. A.; El-Assaad, F.; Aitken, J. B.; Levina, A.; Cohen, D. D.; Siegele, R.; Carter, E. A.; Grau, G. E.; Hunt, N. H.; Lay, P. A., Chemical alterations to murine brain tissue induced by formalin fixation: implications for biospectroscopic imaging and mapping studies of disease pathogenesis. *Analyst* **2011,** *136* (14), 2941-2952.

57.   Chwiej, J.; Szczerbowska-Boruchowska, M.; Lankosz, M.; Wojcik, S.; Falkenberg, G.; Stegowski, Z.; Setkowicz, Z., Preparation of tissue samples for X-ray fluorescence microscopy. *Spectrochimica Acta Part B: Atomic Spectroscopy* **2005,** *60* (12), 1531-1537.

58.   Schrag, M.; Dickson, A.; Jiffry, A.; Kirsch, D.; Vinters, H. V.; Kirsch, W., The effect of formalin fixation on the levels of brain transition metals in archived samples. *BioMetals* **2010,** *23* (6), 1123-1127.

59.   Hare, D. J.; George, J. L.; Bray, L.; Volitakis, I.; Vais, A.; Ryan, T. M.; Cherny, R. A.; Bush, A. I.; Masters, C. L.; Adlard, P. A., The effect of paraformaldehyde fixation and sucrose cryoprotection on metal concentration in murine neurological tissue. *J. Anal. At. Spectrom.* **2014,** *29* (3), 565-570.

60.   Bishop, D. P.; Cole, N.; Zhang, T.; Doble, P. A.; Hare, D. J., A guide to integrating immunohistochemistry and chemical imaging. *Chem. Soc. Rev.* **2018,** *47* (11), 3770-3787.

61.   Frederickson, R. E.; Frederickson, C. J.; Danscher, G., In situ binding of bouton zinc reversibly disrupts performance on a spatial memory task. *Behav. Brain Res.* **1990,** *38* (1), 25-33.

62.   Adlard, P. A.; Parncutt, J. M.; Finkelstein, D. I.; Bush, A. I., Cognitive loss in zinc transporter-3 knock-out mice: a phenocopy for the synaptic and memory deficits of Alzheimer's disease? *The Journal of Neuroscience* **2010,** *30* (5), 1631-1636.

63.   Adlard, P. A.; Sedjahtera, A.; Gunawan, L.; Bray, L.; Hare, D.; Lear, J.; Doble, P.; Bush, A. I.; Finkelstein, D. I.; Cherny, R. A., A novel approach to rapidly prevent age-related cognitive decline. *Aging Cell* **2014,** *13* (2), 351-359.

64.   Suh, S. W.; Jensen, K. B.; Jensen, M. S.; Silva, D. S.; Kesslak, P. J.; Danscher, G.; Frederickson, C. J., Histochemically-reactive zinc in amyloid plaques, angiopathy, and degenerating neurons of Alzheimer's diseased brains. *Brain Res.* **2000,** *852* (2), 274-278.

65.   Lins, B. R.; Pushie, J. M.; Jones, M.; Howard, D. L.; Howland, J. G.; Hackett, M. J., Mapping Alterations to the Endogenous Elemental Distribution within the Lateral Ventricles and Choroid Plexus in Brain Disorders Using X-Ray Fluorescence Imaging. *PLoS One* **2016,** *11* (6), e0158152.

66.   Davies, K. M.; Hare, D. J.; Bohic, S.; James, S. A.; Billings, J. L.; Finkelstein, D. I.; Doble, P. A.; Double, K. L., Comparative Study of Metal Quantification in Neurological Tissue Using Laser Ablation-Inductively Coupled Plasma-Mass Spectrometry Imaging and X-ray Fluorescence Microscopy. *Anal. Chem.* **2015,** *87* (13), 6639-6645.

67.   Hackett, M. J.; Hollings, A.; Caine, S.; Bewer, B. E.; Alaverdashvili, M.; Takechi, R.; Mamo, J. C. L.; Jones, M. W. M.; de Jonge, M. D.; Paterson, P. G.; Pickering, I. J.; George, G. N., Elemental characterisation of the pyramidal neuron layer within the rat and mouse hippocampus. *Metallomics* **2019,** *11*, 151-165.

68.   Chwiej, J.; Janeczko, K.; Marciszko, M.; Czyzycki, M.; Rickers, K.; Setkowicz, Z., Neuroprotective action of FK-506 (tacrolimus) after seizures induced with pilocarpine: quantitative and topographic elemental analysis of brain tissue. *JBIC Journal of Biological Inorganic Chemistry* **2010,** *15* (2), 283-289.

69.   Hackett, M. J.; Britz, C. J.; Nichol, H.; Paterson, P. G.; Pickering, I. J.; George, G. N., In situ Bio-Spectroscopic Investigation of Rapid Ischemic and Post-mortem Induced Biochemical Alterations in the Rat Brain. *ACS Chem. Neurosci.* **2015,** *6*, 226-238.

70.   Ryan, C., Quantitative trace element imaging using PIXE and the nuclear microprobe. *International Journal of Imaging Systems and Technology* **2000,** *11* (4), 219-230.

71.   Ryan, C.; Siddons, D.; Kirkham, R.; Li, Z.; de Jonge, M.; Paterson, D.; Kuczewski, A.; Howard, D.; Dunn, P.; Falkenberg, G., MAIA X-ray fluorescence imaging: capturing detail in complex natural samples. *Journal of Physics: Conference Series* **2014,** *499* (1), 012002.

72.   Webb, S. M., The MicroAnalysis Toolkit: X-ray Fluorescence Image Processing Software. *THE 10TH INTERNATIONAL CONFERENCE ON X‐RAY MICROSCOPY* **2011,** *1365*, 196-199.

73.   Szczerbowska-Boruchowska, M., Sample thickness considerations for quantitative X-ray fluorescence analysis of the soft and skeletal tissues of the human body – theoretical evaluation and experimental validation. *X-Ray Spectrom.* **2012,** *41* (5), 328-337.

74.   Palmiter, R. D.; Cole, T. B.; Quaife, C. J.; Findley, S. D., ZnT-3, a putative transporter of zinc into synaptic vesicles. *Proceedings of the National Academy of Sciences* **1996,** *93* (25), 14934-14939.

75. Chang, C. J.; Nolan, E. M.; Jaworski, J.; Burdette, S. C.; Sheng, M.; Lippard, S. J., Bright Fluorescent Chemosensor Platforms for Imaging Endogenous Pools of Neuronal Zinc. *Chem. Biol.* **2004,** *11* (2), 203-210.

76. Hallman, P. S.; Perrin, D. D.; Watt, A. E., The computed distribution of copper(II) and zinc(II) ions among seventeen amino acids present in human blood plasma. *Biochem. J.* **1971,** *121* (3), 549-555.

H&E Histology

A
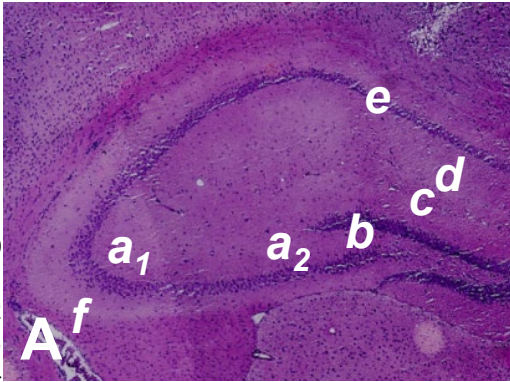
a = CA3 stratum lucidum (mossy fibres)
b = DG granule neurons
c = DG molecular layer
d = CA1 stratum radiatum
e = CA1 pyramidal neurons
f = hippocampus / alveus white matter interface
DG = dentate gyrus
CA = cornus ammonis

Zn Areal Density (ng cm^{-2})
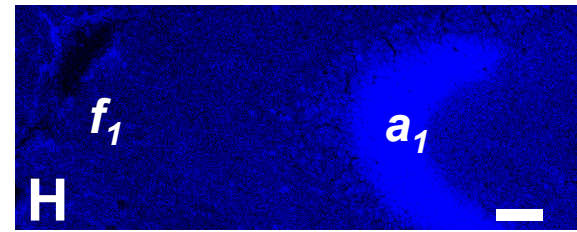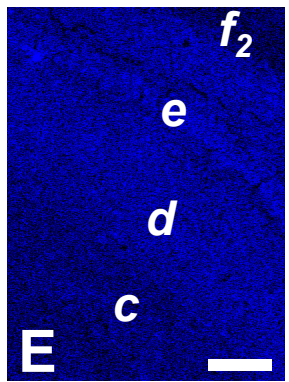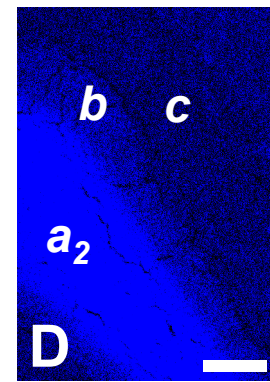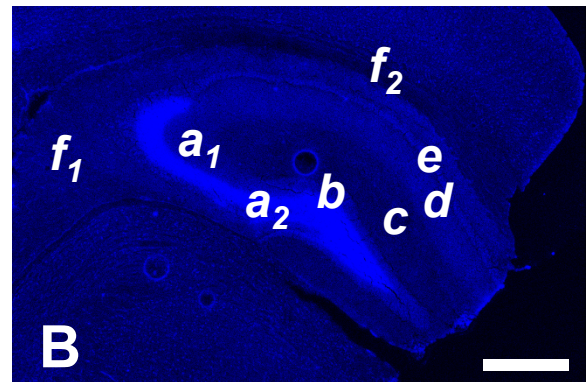
0 — 40

Plunge Freezing in Liquid N$_2$ Cooled Isopentane

B

D

E

H

Formalin Fixed & Sucrose Cryo-Protected

C

F

G

I
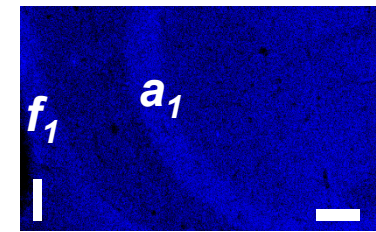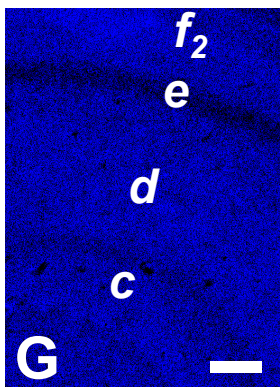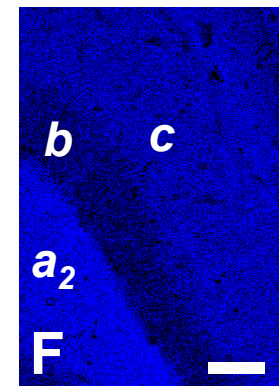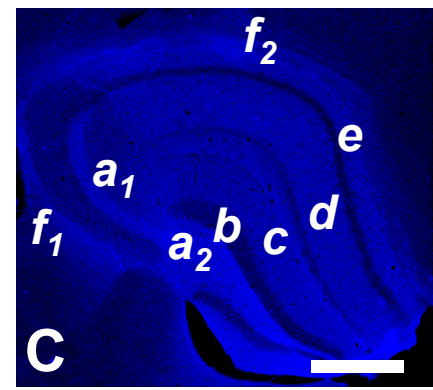
Figure 1: Hippocampal Zn distribution in mouse brain tissue (animal replicate 1) prepared via rapid plunge freezing in liquid-nitrogen-cooled-isopentane (RPF), or sucrose cryo-protection (SCP). (**A**) H&E histology showing the major anatomical sub-regions (*a – f*). (**B, C**) Overview of Zn distribution in hippocampus in tissue prepared via RPF (**B**) or SCP (**C**). (**D – I**) A zoomed in view of Zn distribution in specific anatomical sub-regions of tissue prepared via RPF (**D, E, H**) or SCFP (**F, G, I**). Hippocampal sub-regions are defined alongside H&E histology.
Scale bar in B, C = 500 µm, and D – H = 100 µm.

Plunge Freezing in Liquid N₂ Cooled Isopentane
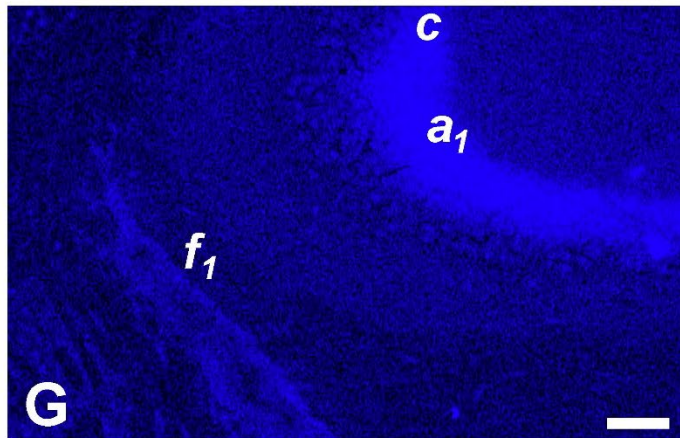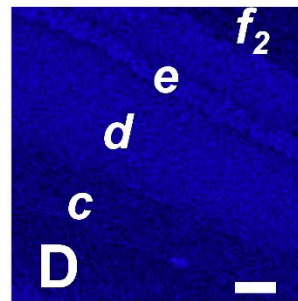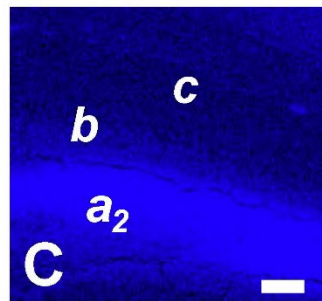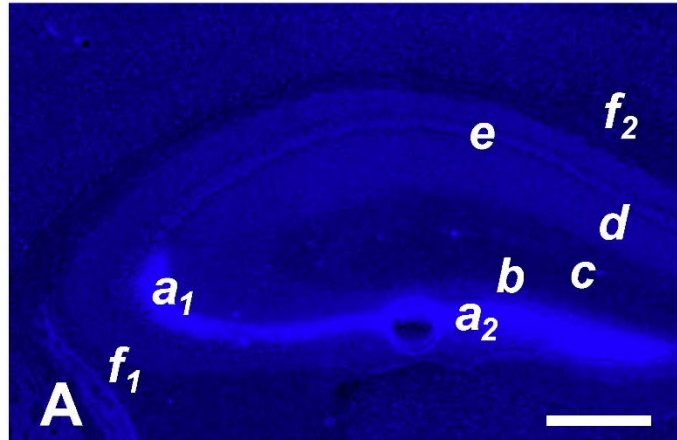
Formalin Fixed & Sucrose Cryo-Protected

Zn Areal Density (ng cm⁻²)

0 40

Zn Areal Density (ng cm⁻²)

0 40
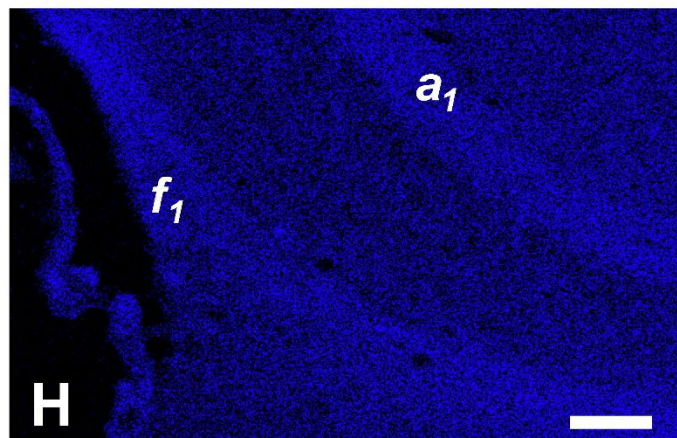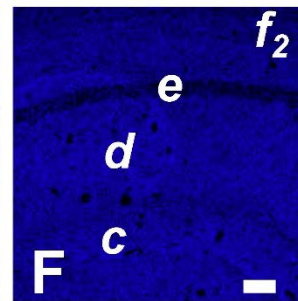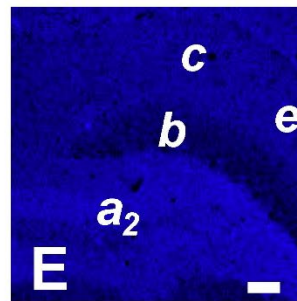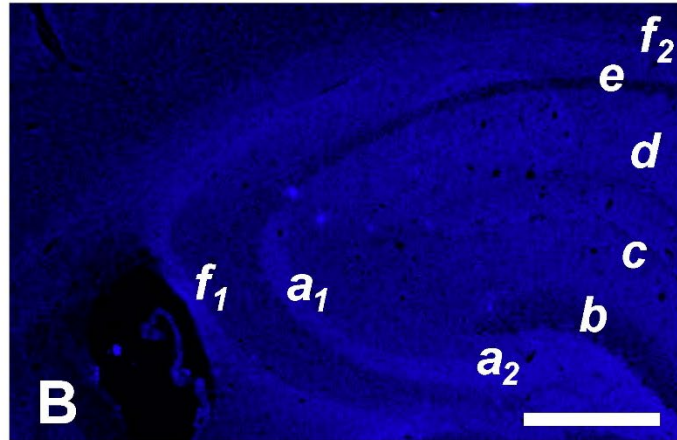
Figure 2: Hippocampal Zn distribution in mouse brain tissue (animal replicate 2) prepared via rapid plunge freezing in liquid-nitrogen-cooled-isopentane (RPF), or sucrose cryo-protection (SCP). (**A, B**) Overview of Zn distribution in hippocampus of tissues prepared via RPF (**A**) or SCP (**B**). (**C-H**) Zoomed in view of Zn distribution in specific anatomical sub-regions of tissue prepared via RPF (**C, D, G**) or SCFP (**E, F, H**). Hippocampal sub-regions are defined in Figure 1, alongside H&E histology. Scale bar in B, C = 500 μm, and D-H = 100 μm.

A Sucrose Cryo-Protection (SCP)

B Rapid Plunge Freezing (RPF)

C SCP / RPF — Relative Zn Content (AU) vs Distance (µm); White Matter (f_1), CA3 Mossy Fibres (a_1)

D SCP / RPF — Relative Zn Content (AU) vs Distance (µm); Dentate Gyrus Molecular Layer (c), Hippocampal Fissure, CA1 Stratum Radiatum (d), CA1 Pyramidal Neuron Layer (e)
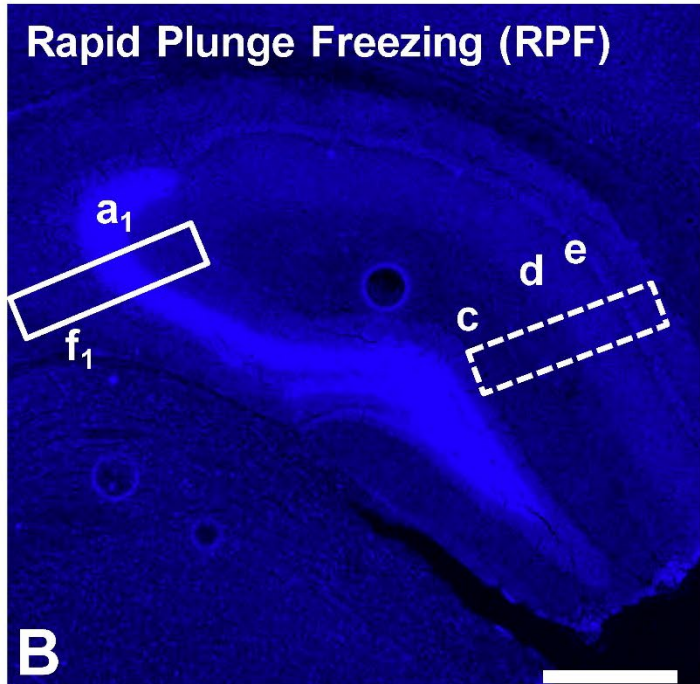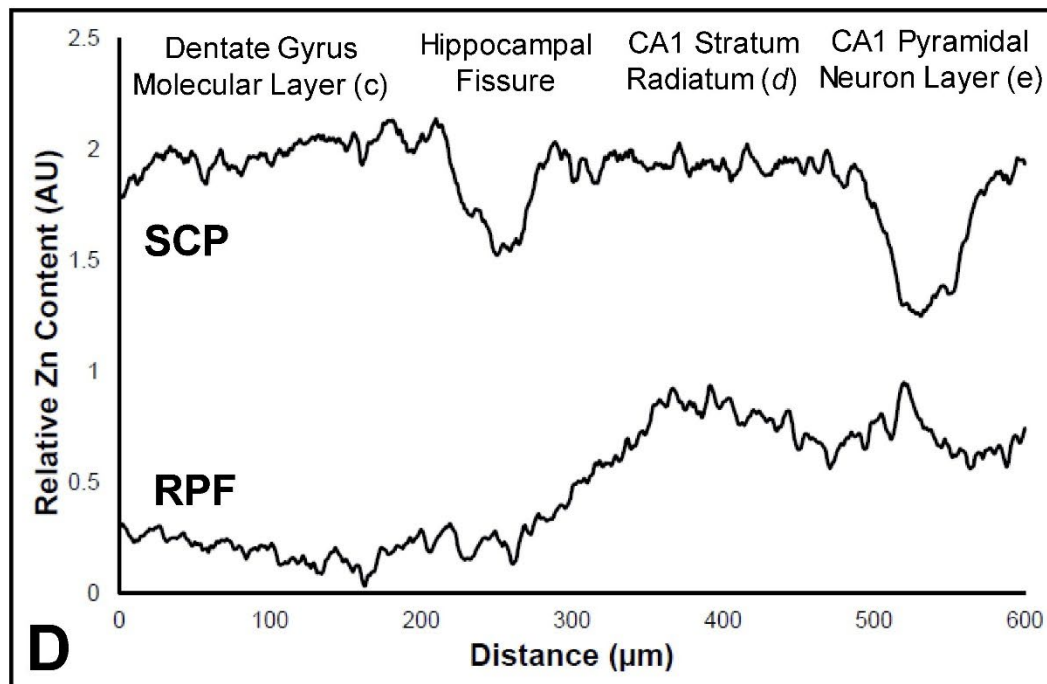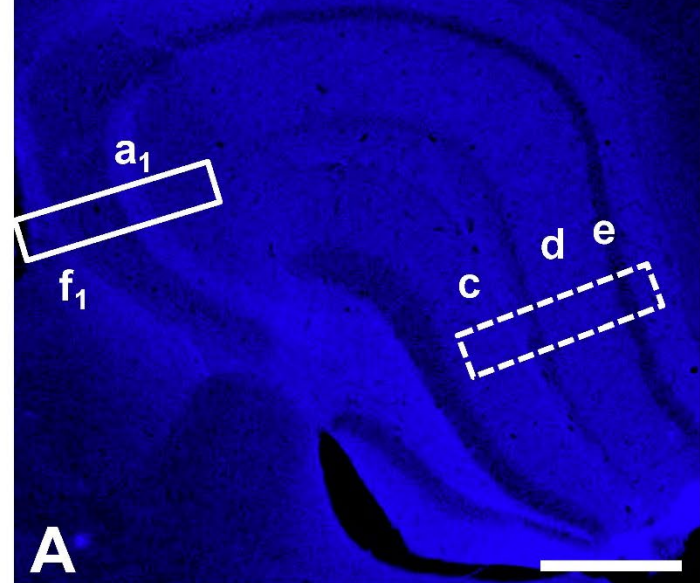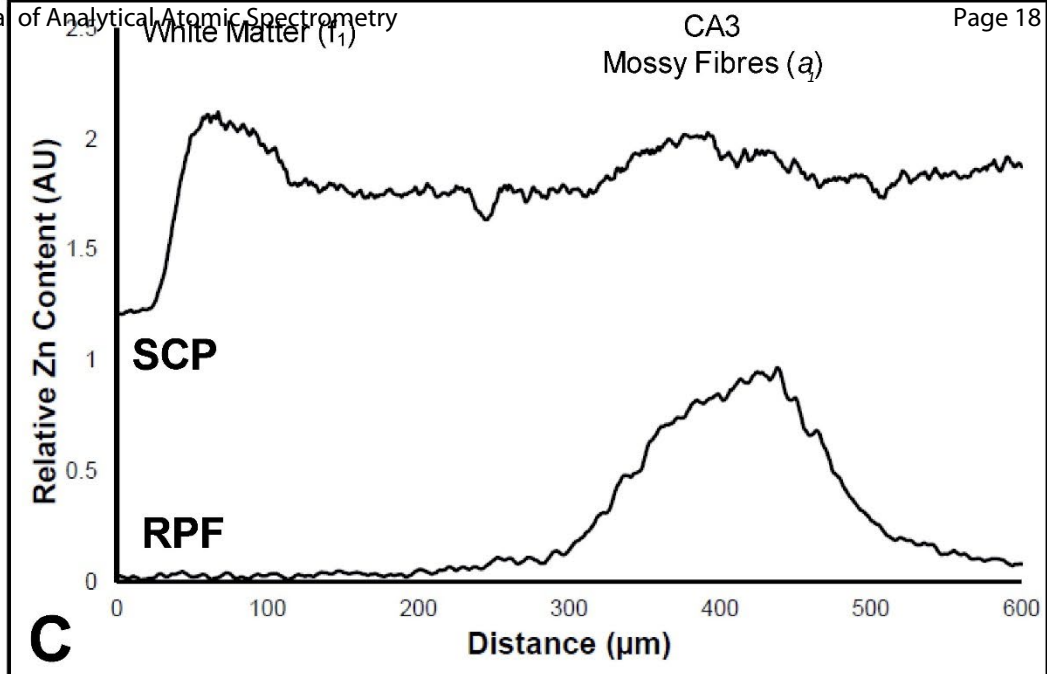
Figure 3: Line profiles of relative Zn concentration throughout mouse hippocampus sub-regions (Zn concentration has been normalised to a max value of 1, and SCP trace offset from the RPF trace, for clarity). The plots highlight the extent of Zn redistribution that occurs in tissues prepared via SCP relative to RPF. (**A,B**) Zn distribution in tissue prepared via SCP (**A**) and RPF (**B**), as also shown in Figure 1. White boxes show regions of interest for line-profiles; Solid box = transect through alveus white matter (f_1) and mossy fibres (a_1). Dashed box = transect through dentate gyrus molecular layer (c), CA1 stratum radiatum (d), and CA1 pyramidal layer (e). (**C, D**) line transects of relative Zn concentration through regions defined by the solid white boxes (**C**), and dashed white boxes (**D**).

Hippocampal sub-regions are defined in Figure 1, alongside H&E histology. Scale bar in A, B = 500 µm.

Plunge Freezing in Liquid N$_2$ Cooled Isopentane

Formalin Fixed & Sucrose Cryo-Protected

Rat 1

Rat 2

Areal Density

100 ng cm^{-2}

10 ng cm^{-2}
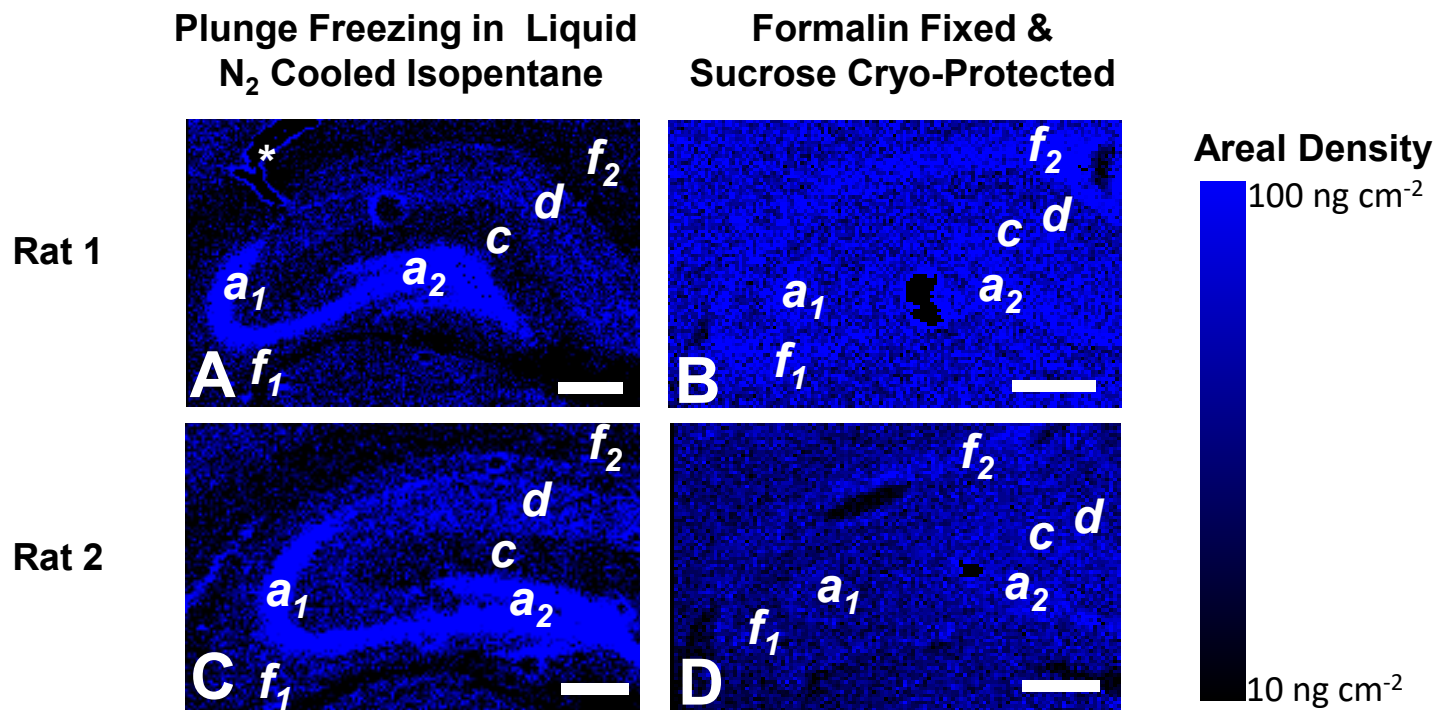
Figure 4: Zn distribution in hippocampal sub-regiongs (*a-f*) within rat brain tissue from two animal replicates, for tissue prepared via (**A, C**) rapid plunge freezing in liquid-nitrogen-cooled-isopentane (RPF), or (**B, D**) sucrose cryo-protection (SCP). Hippocampal sub-regions are defined in Figure 1, alongside H&E histology. Scale bar in A – D = 500µm.
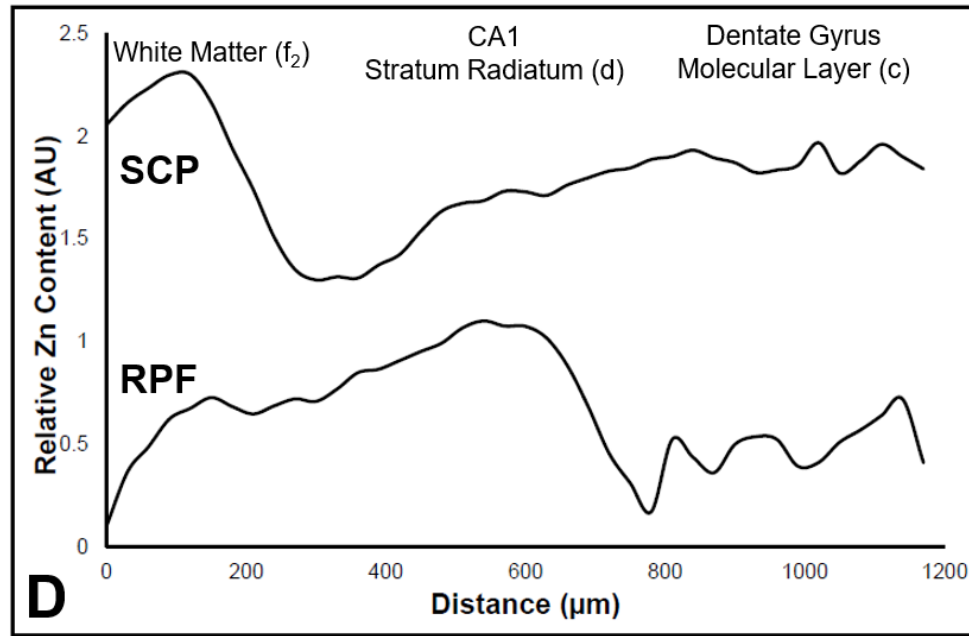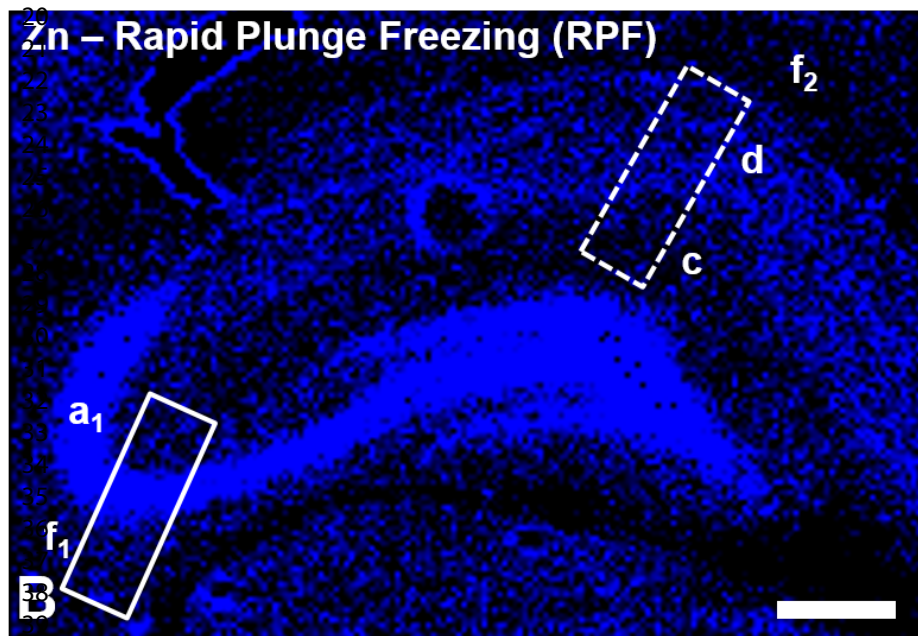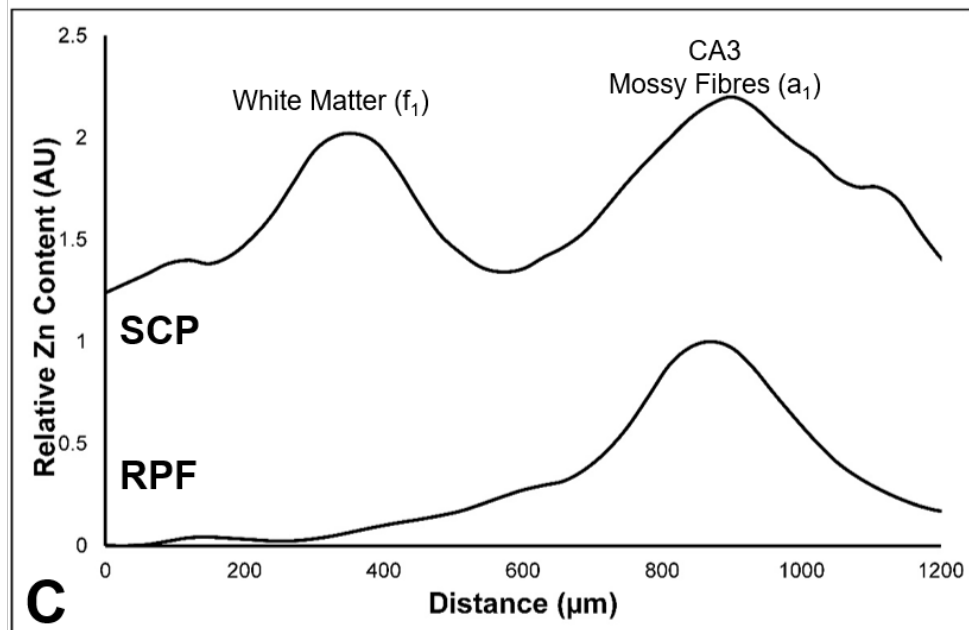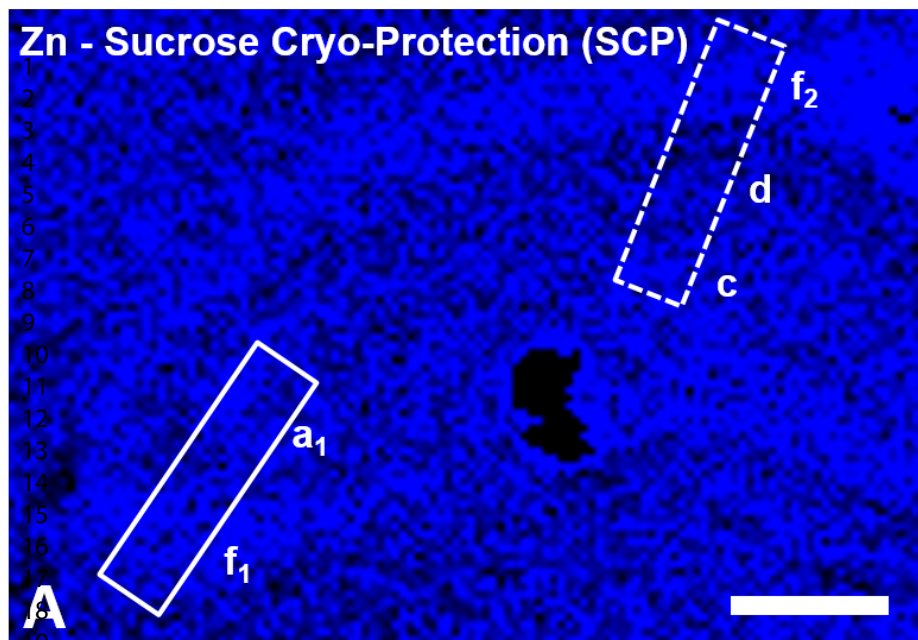
Figure 5: Line profiles of relative Zn concentration throughout rat hippocampus sub-regions (Zn concentration has been normalised to a max value of 1, and SCP trace offset from the RPF trace, for clarity). The plots highlight the extent of Zn redistribution that occurs in tissues prepared via SCP relative to RPF. (**A, B**) Zn distribution in tissue prepared via SCP (**A**) and RPF (**B**), as also shown in Figure 1. White boxes show regions of interest for line-profiles; Solid box = transect through alveus white matter (f_1) and mossy fibres (a_1). Dashed box = transect through dentate gyrus molecular layer (c), CA1 stratum radiatum (d), CA1 pyramidal layer (e), and CA1 corpus callous (f_2) (**C, D**) line transects of relative Zn concentration through regions defined by the solid white boxes (**C**), and dashed white boxes (**D**).

Hippocampal sub-regions are defined in Figure 1, alongside H&E histology. Scale bar in A, B = 500 μm.